Published in Contributions to Mineralogy and Petrology 99, issue 4, 416-429, 1988
which should be used for any reference to this work

Fluid regimes in the deformation of the Helvetic nappes, Switzerland, as inferred from stable isotope data

Martin Burkhard[1] **and Robert Kerrich**[2]

[1] Institut de Géologie, rue E. Argand 11, Université de Neuchâtel, CH-2000 Neuchâtel, Switzerland
[2] Department of Geological Sciences, University of Saskatchewan, Saskatoon, Canada, S7N OWO

Abstract. The stable isotope composition of veins, pressure shadows, mylonites and fault breccias in allochthonous Mesozoic carbonate cover units of the Helvetic zone show evidence for concurrent closed and open system of fluid advection at different scales in the tectonic development of the Swiss Alps. Marine carbonates are isotopically uniform, independent of metamorphic grade, where $\delta\,^{13}C = 1.5 \pm 1.5$ (1 σ) and $\delta\,^{18}O = 25.4 \pm 2.2$ (1 σ). Total variations of up to 2‰ in $\delta\,^{13}C$ and 1.5‰ in $\delta\,^{18}O$ occur over a cm scale. Calcite in pre- (Type I) and syn- tectonic (Type II) vein arrays and pressure shadows are mostly in close isotopic compliance with the matrix calcite, to within ±0.5‰, signifying isotopic buffering of pore fluids by host rocks during deformation, and closed system redistribution of carbonate over a cm to m scale. This is consistent with microstructural evidence for pressure solution – precipitation deformation.

Type III post-tectonic veins occur throughout 5 km of structural section, extend several km to the basement, and accommodate up to 15% extension. Whereas the main population of Type III veins is isotopically undistinguishable from matrix carbonates, calcite in the largest of these veins is depleted in ^{18}O by up to 23‰ but acquired comparable $\delta\,^{13}C$ values. This generation of veins involved geopressurized hydrothermal fluids at 200 to 350° C where $\delta\,^{18}O\ H_2O = -8$ to $+20$‰, representing variable mixtures of ^{18}O enriched pore and metamorphic fluids, with ^{18}O depleted meteoric water. Calc-mylonites ($\delta\,^{18}O = 25$ to 11‰) at the base of the Helvetic units, and syntectonic veins from the frontal Pennine thrust are characterized by a trend of ^{18}O depletion relative to carbonate protoliths, due to exchange with an isotopically variable reservoir ($\delta\,^{18}O\ H_2O = 20$ to 4‰). The upper limiting value corresponds to carbonate-buffered pore fluid, whereas the lower value is interpreted as ^{18}O-depleted formation brines tectonically expelled at lithostatic pressure from the crystalline basement. Carbonate breccias in one of the large scale late normal faults exchanged with infiltrating ^{18}O-depleted meteoric surface waters ($\delta\,^{18}O = -8$ to -10‰).

During the main ductile Alpine deformation, individual lithological units and associated tectonic vein arrays behaved as closed systems, whereas mylonites along thrust faults acted as conduits for tectonically expelled lithostatically pressured reservoirs driven over tens of km. At the latest stages, marked by 5 to 15 km uplift and brittle deformation, low ^{18}O meteoric surface waters penetrated to depths of several km under hydrostatic gradients.

Offprint requests to: M. Burkhard

Introduction

Stable isotope studies have been widely applied to monitor fluid- related processes in the earth's crust (see Hoefs 1973, 1987; Valley et al. 1986; Kyser 1987 for general reviews and extensive references). It is generally agreed that stable isotope signatures may provide critical information concerning fluid sources, fluid flow, and exchange reactions between fluids and rocks. However, only a few stable isotope studies have been undertaken in orogenic belts, including the Alps, to address the specific question of the interrelationship between deformation and fluid advection (Baertschi 1957; Hoefs and Frey 1976; Frey et al. 1976; Hoefs and Stalder 1977; Kerrich et al. 1978; Kerrich and Rehrig 1987; Hoernes and Friedrichsen 1978, 1980; Dietrich et al. 1983; Weissert and Bernoulli 1984; Taylor and Bucher-Nurminen 1986).

In the Helvetic zone of the Swiss Alps, the activity of fluids during deformation is clear in most outcrops, marked by numerous generations of syntectonic veins and pressure shadows. The aim of this study was to use stable isotope analyses of well characterized structures on a cm to km scale, in order to establish the interrelationships between fluid regimes, structures and deformation mechanisms during tectonic development of the Helvetic Alps. In particular, we have attempted to test for evidence of open or closed system material and fluid behaviour in successive generations of vein arrays, and for large scale advection through major thrust faults. Tectonically driven advection of fluids is anticipated in the Helvetic and Pennine nappes from a consideration of their position within the Alpine chain as a whole (see Etheridge et al. 1983, 1984; Fyfe and Kerrich 1985; Oliver 1986; Kerrich 1986; Kerrich and Rehrig 1987). Pore-water expelled from initially fluid saturated sediments, structural water, and CO_2 released from silicate-carbonate or decarboxylation reactions during prograde metamorphism in the footwall of a thrust structure are possible fluid sources, as well as deep penetration of surface meteoric water from a topographically elevated mountain chain.

Previous reconnaissance studies of the Helvetic Alps have shown that syntectonic quartz-carbonate vein arrays

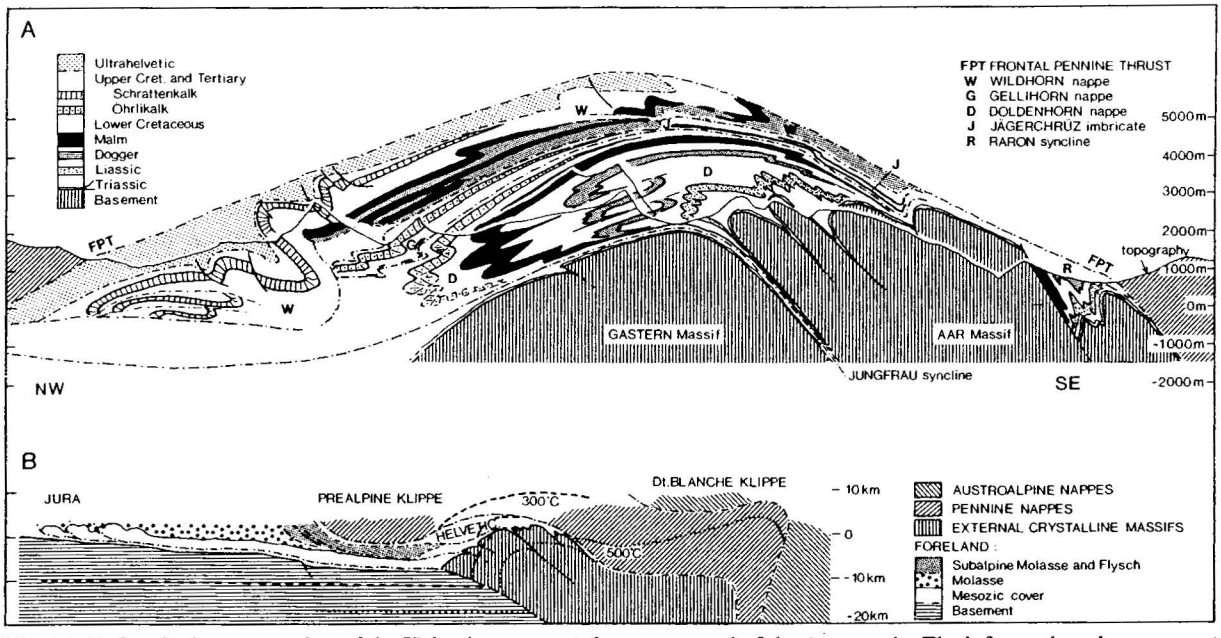

Fig. 1 A, B. Synthetic cross-section of the Helvetic nappes at the western end of the Aar massiv. The information above current topographic levels is constructed by projecting from the west side along plunging fold-axes with a maximum projection distance of 15 km. **B** Profile showing the setting of section **A** within a complete tectonic cross-section of the western Alps (simplified after Trümpy 1980), and with estimated metamorphic temperatures superposed

formed in essentially closed systems, in isotopic equilibrium with the adjacent rock-matrix (Kerrich et al. 1978), a situation classically termed pressure-solution (see Durney and Ramsay 1974). Dietrich et al. (1983) also identified a close compliance between the O and C isotopic compositions of syntectonic veins and their adjacent wall-rocks. However, in a series of up to five generations, the earlier veins were slightly depleted in ^{13}C (up to 1.5‰) with respect to their matrix, and this was interpreted to indicate a component of open system behaviour at the onset of the tectonic history which became closed in the final stages.

Tectonic setting

A synthetic cross-section of the study-area is presented in Fig. 1 A illustrating the relationships between the different units. Highly detailed deformational scenarios for the tectonic evolution of the Helvetic part of the Alps have been clearly formulated (Milnes and Pfiffner 1980; Laubscher 1983; Mugnier and Ménard 1986; Burkhard 1988). A summary for the western part of the Helvetic nappes is given in Table 1, with particular emphasis on placing the different types and generations of structures analyzed into the larger tectonic and time framework.

Metamorphic zonation within the Helvetic nappes has been successfully established by a combination of illite crystallinity, clay mineralogy, coal rank and fluid inclusion studies (Durney 1972; Poty et al. 1974; Hoefs and Stalder 1977; Mullis 1979, 1987; Kübler et al. 1979; Frey et al. 1980; Frey 1986; Burkhard 1988). Mullis (1979) mapped three successive fluid zones characterized by higher hydrocarbons, CH_4 and H_2O respectively which correspond to diagenesis ($T<200°$ C), low and medium anchizone, and higher anchi- and epizone ($T>270°$ C) respectively; CO_2 may be present in small amounts in all fluid zones (see also Hoefs and Frey 1976; Hoefs and Stalder 1977).

The structural style within the different Helvetic nappes is mainly controlled by the metamorphic grade. Brittle to semi-brittle deformation is dominant in the diagenetic upper Helvetic units, whereas more ductile deformation is found in the Morcles-Doldenhorn-nappe which deformed partly under greenschist facies conditions. This nappe is characterized by its large inverted limb, and significantly this is the only unit in the Helvetic sequence containing a crystalline core derived from the Aar massif.

The position of the Helvetic nappes within the Swiss Alps as a whole is shown at a larger scale in the lower cross-section (Fig. 1 B). The schematically indicated isograds for 300 and 500° C show that considerable transported metamorphism occurred along the frontal Pennine thrust (i.e. Frey 1986). This feature underlines the importance of this thrust as a major and long-lived structure, and is particularly relevant for understanding the deformation of the Helvetic nappes which are bounded between 5 to 10 km of Pennine nappes in the roof ("orogenic lid" Laubscher 1983) and the crystalline basement in the footwall.

Lithologies and structures analyzed

Evidence for syntectonic crystallization of calcite and quartz (minor dolomite, ankerite, albite and many other minerals) from a fluid phase in tectonic structures is widespread in all of the Helvetic nappes. In order to obtain information about the nature and origin of the fluids involved in the tectonic development of the Helvetic nappes, C and O isotope compositions of carbonates were analyzed in 125 samples representative of the large variety of different structures from all of the tectonic units represented in the study-area, as described below. Quartz was separated from 12 of these samples for $\delta\,^{18}O$ determinations. Here we emphasize details of the tectonic setting, geometry, scale and evolution of the various structures sampled, as well as the micromechanics of deformation involved, as these factors bear critically on the question of open versus closed system behaviour, and accordingly provide an essential framework for interpretation of the isotopic data.

Veins

Different generations of veins are classified into one of three types according to their relative age within the deformation history of a nappe (Dietrich et al. 1983; Franck et al. 1984; Burkhard 1986). Any given vein is readily recognized as pre- syn- or post-deformational (main-deformation) according to its orientation relative to the schistosity or an axial planar cleavage, and by its state of internal deformation as compared to the surrounding matrix.

Table 1. Deformation phases

Age	Deformation-phase	Large scale structures	Small scale structures
0 Ma	Grindelwald	Uplift/doming of external Crystalline Massifs deep thrusts under crystalline massifs Folding and thrusting of Jura Fold Belt	Brittle deformation related to Late Faults tensile Type III veins perpendicular to fold axes
	Simplon Rhone	Simplon-Fault, extension in E-W direction dextral shearzone in Rhone valley	Pressure shadows, Type II & III veins in root zone of Helvetic nappes
20 Ma	Kiental	Folding and thrusting of Morcles – Doldenhorn *n.* Second deformation of higher Helvetic nappes	Ductile deformation in lower Helvetic units pressure shadows, mylonites, schistosity Type II veins in higher Helvetic units
	Trubelstock	Folding and thrusting of Jägerchrüz- and Plammis imbricates Second folding of southern Wildhorn nappe	Ductile deformation, schistosity, mylonites pressure shadows, Type I veins in lower units Type II veins in Wildhorn nappe
	Prabé	Folding and thrusting of Wildhorn and Gellihorn-nappes	Brittle to semi-brittle deformation, tectonites on thrust planes, Type I & II veins
40 Ma	Plaine Morte	Emplacement of Ultrahelvetic on Wildhorn *n.*	Brittle deformation, Type I veins
		Formation of northern Pennine nappes; their final emplacement continues during the main deformation phases of the Helvetic units	Ductile and brittle deformation according to structural level, Type I veins in schistose horizons
60 Ma 120 Ma	Eo-Alpine	Formation of Austroalpine and southern Pennine nappes, partly high p metamorphism	Not represented in study area

Type I, early veins are parallel with or slightly oblique to the schistosity and bedding (Fig. 2A, B). These veins suffered subsequent deformation, leading to small folds, boudinage and recrystallization of the vein-filling. The most important veins of this set are up to 15 cm thick and several metres long. Smaller veins (mm to cm) are frequent in schistose horizons.

Type II, syntectonic veins, formed at high angles to the schistosity and bedding often in single or conjugate sets of en-echelon arrays (Fig. 2C). Single veins are usually restricted to one layer, and are typically a few mm to a few cm thick and dm to some metres in length. The mineralogy of these veins closely reflects the mineralogy of the surrounding matrix. Syntectonic veins may be related to the folding, thrusting and different types of faults. From crosscutting relationships it is possible locally to subdivide further the syntectonic veins into successive vein-arrays.

Type III late tectonic tensile veins formed at high angles to the schistosity and bedding, perpendicular to the foldaxial trends (Fig. 3D, E). These veins crosscut all the previous vein generations as well as the schistosity, folds and thrusts. Single veins form throughgoing fractures and may be followed over tens of metres across different layers. The largest of these veins are up to 3 m wide (Furrer and Hügi 1952) and have been termed '*dikes*' by convention to distinguish them from the smaller veins. Veins of Type III form a distinct array of regularly oriented planar tectonic elements and have a geomorphological expression on the 1:25,000 maps as well as being visible on aerial photographs. The extension related to this particular vein-system is typically a few percent, but up to 15% stretching can be found locally (Dietrich et al. 1983).

Secor (1965) has shown that tensile fractures require either a shallow depth of formation or increased fluid pressure relative to the hydrostatic pressure gradient (see also Etheridge 1983). In the case of the Type III examples described here, the possibility of a shallow depth can be ruled out for several reasons: Type III veins occur throughout the entire thickness of the Helvetic nappes which corresponds to a vertical relief of more than 5 km. From the orientation of the latest veins it seems that they are tilted according to the general plunge-vector of the external crystalline massifs (Burkhard 1986, Fig. 6). Mullis 1979, 1987 determined temperatures which closely reflect peak metamorphic conditions of the surrounding wallrocks from quartz fluid inclusions of this generation of veins. Consequently, it is necessary to postulate ambient fluid pressures in excess of hydrostatic.

Pressure shadows are a characteristic deformation feature of lower greenschist facies metamorphic conditions where calcite and/or quartz-fibres are frequently found as beards on rigid objects such as pyrite-grains, or as infillings between fragmented segments of boudinaged belemnites (Durney 1972; Ramsay and Huber 1983). Veining in these areas generally does not occur during peak metamorphic/deformational conditions, but rather pre- or postdates the main deformation. Exceptions are veins within competent boudinaged layers (Fig. 2F). On the other hand, pressure shadows do not occur within the diagenetic to anchizonal higher Helvetic nappes (Burkhard 1986).

Thrusts

From the micro-structural/mechanical standpoint, two different types of thrusts can be distinguished within the Helvetic nappes: higher thrusts follow shaly horizons and pressure solution/crystallization phenomena are predominant, leading to strongly tectonized "veinites" at the thrust contact (Fig. 3A, B). In contrast, the lower Helvetic Doldenhorn-Morcles-nappe has a strongly attenuated but continuous inverted limb (Fig. 3C, D) which can be followed into a narrow thrust zone, the Jungfrau- Chamonix- syncline (Fig. 1). Calc-mylonites from this horizon show ample evidence for crystal plastic deformation and dynamic recrystallization (Schmid et al. 1981; Schmid 1982). The Lochseiten calc-mylonite of the Glarus overthrust in eastern Switzerland has accomodated in excess of 20 km displacement within a one metre thick horizon. Super plastic deformation mechanisms are thought to be responsible for the high strains (Schmid et al. 1981; Schmid 1982; Pfiffner 1982).

Pressure solution seams and highly deformed veins are ubiquitous in both outcrops and thin-sections from different samples of the Lochseiten calc-mylonite and the Morcles- Doldenhorn- thrust (Fig. 3D, E)). Dynamic recrystallization phenomena occur in both vein and matrix calcite signifying that the veining took place simultaneously with thrusting and microstructure development. In addition to the importance of the solid state recrystallization phenomena stressed by the authors cited above, the (micro-)veins and stylolithes are clear evidence for the presence of a fluid phase during the enhanced ductility that accommodated deformation and thrust-

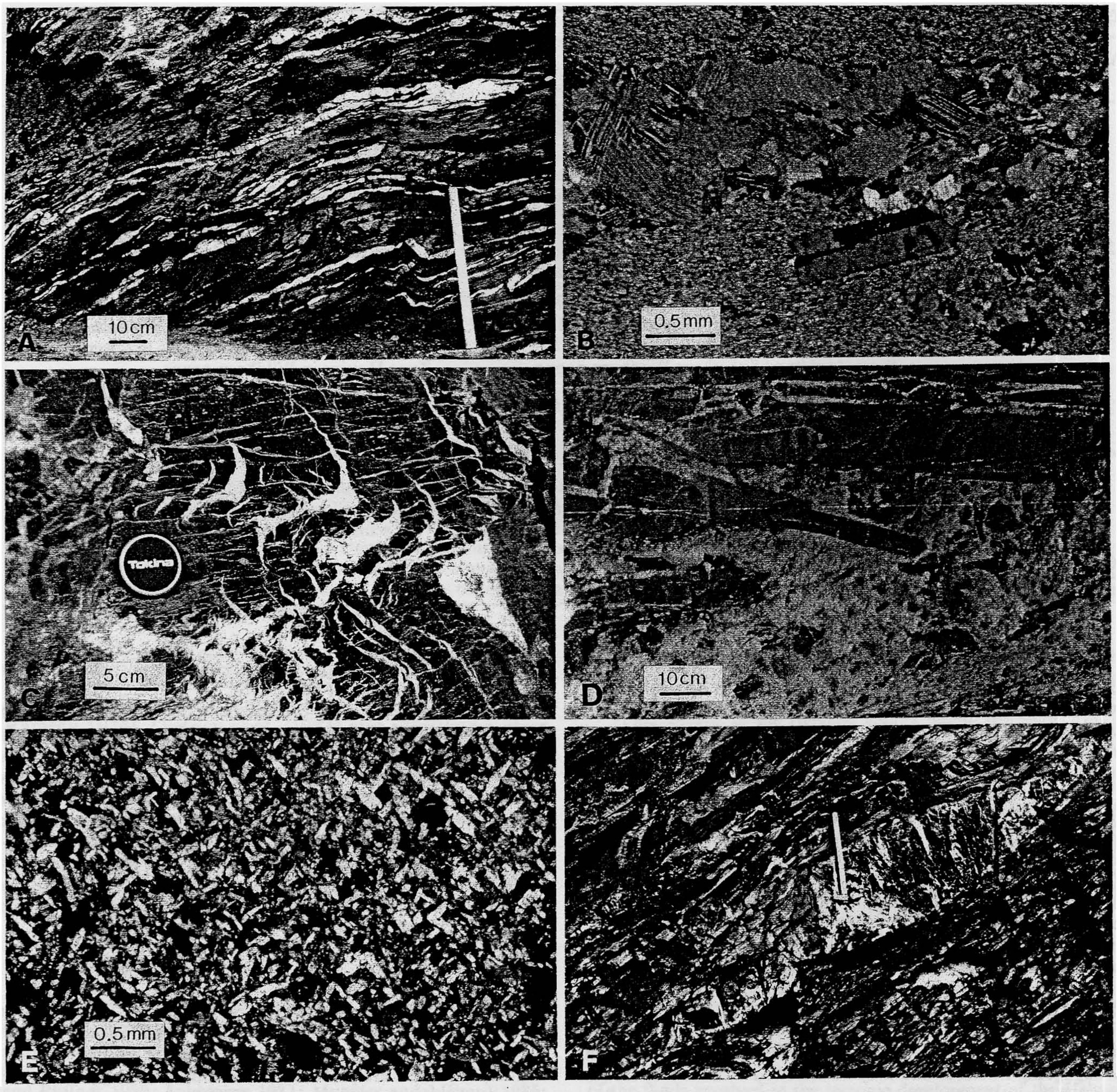

Fig. 2. **A** Type I veins in Malm limestone at Leuk, locality no. 5. **B** Microphotograph, crossed nicols, Type I microvein at the same locality as A. Note intensely twinned calcite and secondary albite. **C** Type II veins in Malm limestone of Wildhorn nappe at Lämmernhütte, sample locality no. 27. **D** 'Calcite dike' (Type III vein) in Malm of Doldenhornnappe, sample no. 32. **E** Microphotograph, crossed polars, of 'quartz dike' (Type III vein) in Tertiary of Doldenhornnappe at Trublen, sample no. 33. **F** Veins in boudinaged competent layer of dolomitic limestone within strongly flattened Malm limestone, Jägerchrüz imbricate at Leuk

ing. This fluid might also have played an important role in the thrust deformation by influencing the magnitude of normal stress on the thrust-planes, and thus frictional sliding resistance. As Kerrich et al. (1977), Kerrich (1978), Schmid (1982) and numerous other authors have emphasized, conditions of differential stress, strain rate, temperature and grain size may change throughout the tectonic history, such as to induce transitions between deformation regimes dominated by intracrystalline plasticity, intercrystalline processes and pressure solution.

The contact between Helvetic and Pennine units is one of the major thrust structures within the Alps. This thrust follows shaly and evaporitic horizons, and accordingly no extremely deformed unit, or counterpart to the Lochseiten calc-mylonite is known from the Pennine thrust. Limestones are subordinate in the Pennine nappes but carbonate-quartz veins are widespread in all the schistose horizons (Fig. 3F). The largest veins are decimetric in width and a few metres long, sub-parallel to the schistosity; geometrically, they resemble the Helvetic Type I veins. Their formation is probably linked with some stage of thrusting of the Pennine units.

Faults

The formation of late cross-cutting faults in the Helvetic nappes can be related to their post emplacement history. Since the Miocene, up to 15 km of vertical uplift has brought greenschist facies rocks to the surface. This uplift and doming are explained by deep seated thrusting of the external crystalline massifs over the foreland in a complex ramp flat geometry (Burkhard 1988). The response

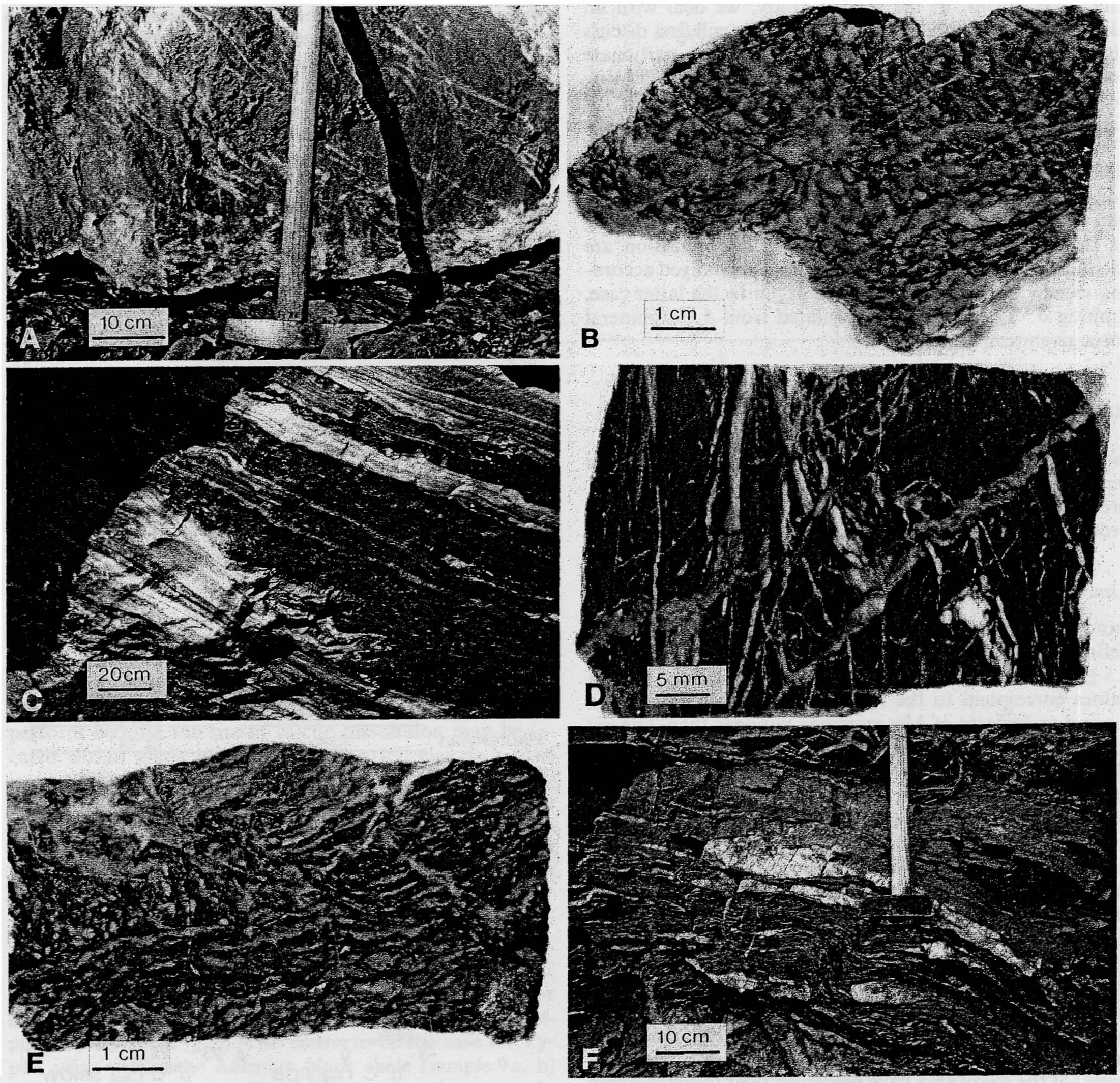

Fig. 3. **A** Close up view of Wildhorn thrust near Kandersteg. Strongly deformed Malm boudin. **B** Polished surface of hand specimen form thrust contact of Wildhorn nappe at Kandersteg, sample no. 52. **C** Detail of inverted limb (thrust zone) of Morcles nappe at Saillon. Initially hecto- to decametric layering of limestones and marls is now tectonically reduced to decimetric bands of calc mylonites, locality no. 55. **D** Polished surface of hand specimen from Doldenhorn thrust. White calcite veins at various intensities of deformation crosscut the calc- mylonite, sample no. 53. **E** Polished surface of Lochseiten calc-mylonite handspecimen from the Glarus thrust at Pizol, sample no. 56. **F** Syntectonic, layer parallel veins in Schistes lustrés near the frontal pennine thrust in Rhone valley, sample no. 73

of the cover to this thrusting are late brittle faults and Type III veins, which both indicate stretching in a SW-NE direction, parallel to the Alpine chain.

Analytical methods

Standard procedures were employed for the extraction of O_2 from quartz using BrF_5 (Clayton and Mayeda 1963) and of CO_2 from carbonate minerals using 100% H_3PO_4 at 25° C (McCrea 1950). For samples in which calcite and dolomite were intimately intergrown, separate analyses were made using timed extractions. Isotopic data are reported in the conventional δ-notation, as ‰ deviations from PDB for carbon, and from SMOW for oxygen. The long-term reproducibility of $\delta\ ^{13}C$ and $\delta\ ^{18}O$ values has averaged 0.18‰ (2 σ).

Open versus closed system

Closed systems are characterized by bulk isotopic composition which remain constant whereas in an open system isotopic composition may be changed by interaction with external isotopic reservoirs (fluids e.g.). Different models of water/rock interaction are discussed at length by Gregory

and Criss (1986). In the present study, we deal with an almost monomineralic (calcite) system. We will first discuss the isotopic composition of the predominant carbonate rocks. This is an essential starting point for the following sections, where potential channelways are examined for signs of isotopic exchange with externally derived fluids. Two different extreme models are considered: If rock $\gg$ fluid, $\delta\ ^{18}O\ H_2O$ will be equilibrated with the rock and consequently any secondary mineralization from this fluid will be isotopically indistinguishable from the rock as long as the temperature of dissolution and crystallization are identical. If rock $\ll$ fluid, $\delta\ ^{18}O$ rock will be changed according to new equilibrium with $\delta\ ^{18}O\ H_2O$. In the latter case, limiting $\delta\ ^{18}O\ H_2O$ can be calculated from $\delta\ ^{18}O$ mineral for a given temperature.

Results and discussion

Isotopic analyses of the Mesozoic marine carbonates are reported first, followed by data for vein-wallrock pairs, pressure shadow-matrix pairs, thrusts and faults, in the order that these various structures were discribed above.

Limestone matrices

Isotopic compositions of the limestones plot within a well-defined field where the average $\delta\ ^{13}C$ and $\delta\ ^{18}O$ values are $1.5 \pm 1.5‰$ (1 σ) and $25.4 \pm 2.2‰$ (1 σ) respectively. Matrix values correspond to the range established as typical for marine carbonates of Mesozoic age younger than Triassic (box outlined in Fig. 4 according to Hoefs 1973 p.97, see also Veizer and Hoefs 1976). No systematic trends between lithologies could be detected (Fig. 5). The largest number of analyses are from the micritic Malm limestones, a seemingly homogeneous unit in composition and texture which displays only minor isotopic variability. The mean and standard deviation for 26 Malm limestones (including 11 values published by Dietrich et al. 1983) are $\delta\ ^{13}C = 1.8‰ \pm 1.1$ (1 σ) and $\delta\ ^{18}O = 25.6‰ \pm 1.8$ (1 σ). Multiple analyses of the matrix and a belemnite from different spots in one sample (42) revealed total variations of up to 2‰ in $\delta\ ^{13}C$ and 1.5‰ in $\delta\ ^{18}O$ (see Fig. 7). Despite these variations, no pronounced excursions in $\delta\ ^{13}C$ or $\delta\ ^{18}O$ from the "marine limestone field" were found, and apparently the limestones of the study area have preserved their initial isotopic composition since the time of deposition and diagenesis.

Hudson (1977) and Tucker (1982) have shown that various different types of carbonate in a sediment may vary isotopically by as much as 12‰ in $\delta\ ^{18}O$ and 4.5‰ in $\delta\ ^{13}C$; and Magaritz (1974) has measured sympathetic shifts of $-5‰$ in $\delta\ ^{18}O$ and $\delta\ ^{13}C$ that accompanied lithification in a freshwater environment. Accordingly, the measured isotopic variability in the limestones may simply be an intrinsic feature of the depositional and diagenetic environments (for reviews see O'Neil 1987). The Mesozoic sediments of the Helvetic area have undergone at least one important phase of exposure at the land surface during late Cretaceous to Tertiary time, which led to the deposition of the "Eocene Bohnerz formation". This formation marks a period of erosion and karstification where deep penetration of freshwater could have occurred. Apparently, this event did not markedly change the isotopic composition of the Mesozoic limestones.

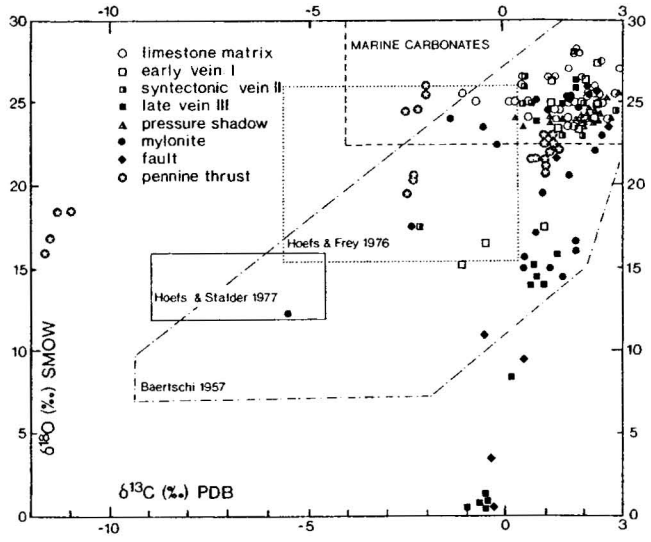

Fig. 4. Isotopic composition of all the analysed carbonate samples plotted in $\delta\ ^{18}O$-$\delta\ ^{13}C$ space. The various different boxes outlined represent fields for marine carbonates according to Hoefs (1973, p.97), for cleft-carbonates from the central Alps (Hoefs and Stalder 1977), for carbonates from the Liassic Quartenschiefer (Hoefs and Frey 1976) and for various carbonates (marbles, veins, clefts) from the central Alps (Baertschi 1957)

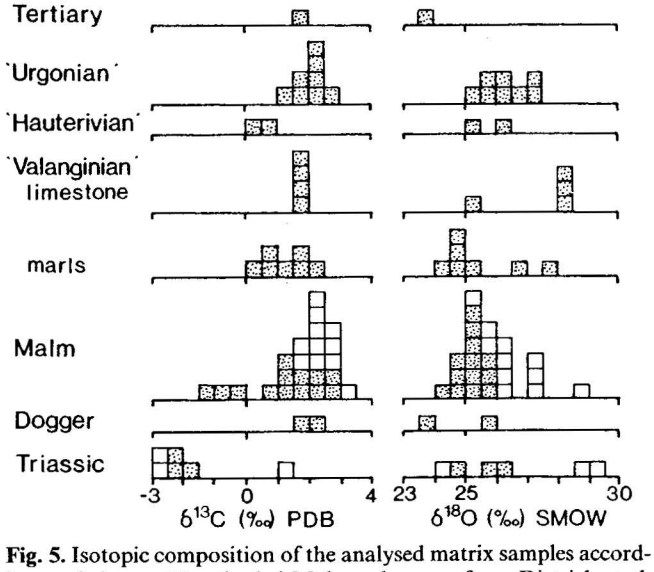

Fig. 5. Isotopic composition of the analysed matrix samples according to their age. Un-stippled Malm values are from Dietrich et al. (1983), un-stippled Triassic values are from Kerrich et al. (1978)

No relationship between the isotopic composition of the limestones and metamorphic grade could be detected. Even strongly metamorphosed Mesozoic limestones from the lower Pennine nappes (marble of Peccia, used as standard by Baertschi 1957) and from the contact aureole of the Bergell intrusion (Taylor and Bucher-Nurminen 1986) collectively plot within the field of "marine limestones", signifying that metamorphic grade *alone* has not disturbed primary sedimentary isotopic signatures.

Veins

Representative veins have been analyzed and compared to their adjacent wallrock. Given that some of the host rocks

may possess a small degree of variability in isotopic composition as described above, individual vein-wallrock pairs are plotted separately in Fig. 6, where the origin represents a "normalized" host rock value and each point is the corresponding vein analysis. Veins of different relative ages from the same outcrop are linked with tie-lines showing the trend from older to younger generations (arrows). From consideration of the different possible sources of error, and the heterogeneity of the matrices (and veins), small differences between veins and their matrices are not necessarily significant in terms of open versus closed system behaviour. We consider analyses for veins that plot within the dashed box ($\pm 0.5‰$ $\delta\,^{18}O$ and $\delta\,^{13}C$) as being isotopically indistinguishable from their matrix (the dashed box could be arbitrarily larger). From Fig. 6 it appears that many veins, regardless of their type (I, II or III), plot within this dashed box.

A slight overall tendency may exist for the veins to plot in the quadrants depleted in ^{13}C and/or ^{18}O with respect to their matrix, but some enriched values also exist. However, any such trend is small (0.5 to 1.5‰) compared to the variability of matrix values ($2\sigma = 3.0$ and 4.4‰ for $\delta\,^{13}C$ and $\delta\,^{18}O$ respectively) and we conclude that rather than the age of any given vein, its size determines the magnitude of isotopic difference relative to the adjacent matrix. We were not able to confirm the results of Dietrich et al. (1983), (square symbols in our Fig. 6) who argued that the earlier veins were formed in a partially open system which became closed during later vein generations. Furthermore, representative sampling of "the host rock" is not easy to perform because the site of calcite dissolution may be located within marly interlayers. As detrital clay in a marl is generally depleted in ^{18}O relative to the carbonate fraction (i.e. Hunziker et al. 1986) the clay could potentially act to drive the pore fluid to lower $\delta\,^{18}O$ than in a pure carbonate sediment. Any syntectonic calcite precipitated under closed system conditions from this pore fluid would also be ^{18}O-depleted relative to the matrix carbonate. Moreover, if the marl contained any ^{13}C-depleted carbonaceous material which underwent oxidation, then the interstitial fluid and syntectonic calcite would acquire lower $\delta\,^{13}C$ values than the sedimentary calcite. This could account for a clustering of vein analyses within the ^{13}C- and ^{18}O- depleted quadrant (Fig. 6). This seems to be the case for Type I veins within the Aalenian black shale (sample 9a, b) which are depleted by ca. 7‰ in ^{18}O compared to the main population of Type I veins and are also marginally depleted in ^{13}C. A similar range of values has been reported by Hoefs and Frey (1976) for Liassic shales (see box in Fig. 4).

Ambient temperatures of pre- syn- and post-tectonic veining are not well constrained. Quartz-calcite pairs from Type I veins (samples 1c, 1d, 3a and 6a; Fig. 9) yield oxygen isotope temperatures of 220, 290, 190 and 260° C respectively. There are no means for testing isotopic equilibrium, but these values are slightly lower than expected from the epizonal grade of the surrounding areas (Burkhard 1988). This disparity could signify that their formation predates peak metamorphic conditions, or alternatively that the calcites have undergone retrograde oxygen isotope exchange. Type II veins are interpreted as synmetamorphic and Type III veins probably formed during decreasing temperatures.

In summary, most of the veins formed in or close to isotopic equilibrium with their adjacent matrix, where the

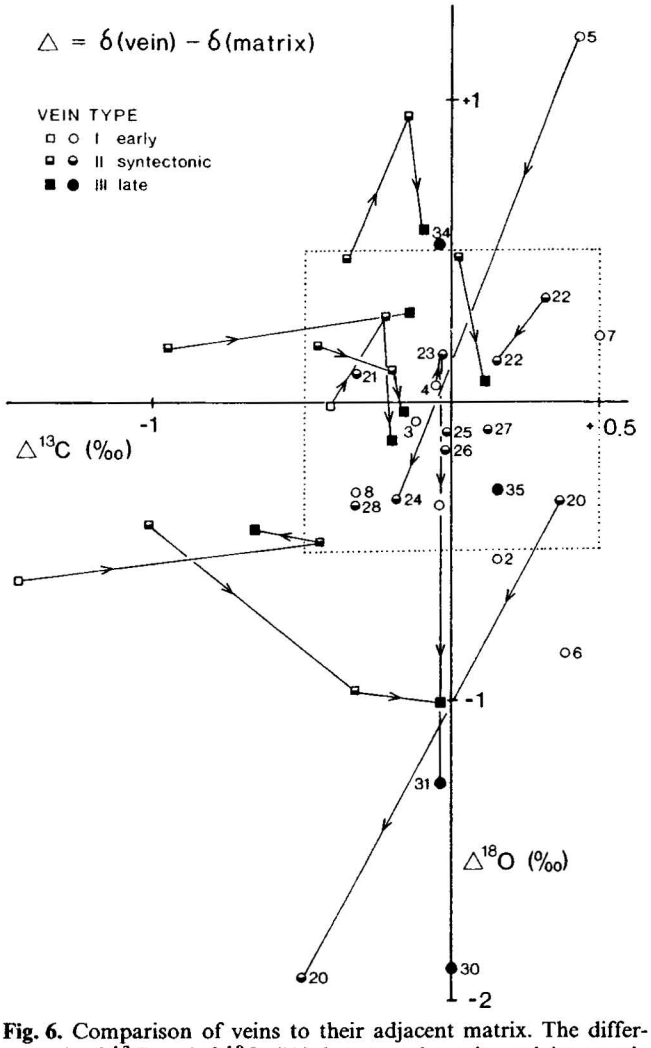

Fig. 6. Comparison of veins to their adjacent matrix. The differences in $\delta\,^{13}C$ and $\delta\,^{18}O$ (‰) between the vein and its matrix are plotted on the x- and y-axes respecively. The origin represents a normalized matrix-value (0, 0) regardless of its absolute isotopic composition. Vein-values falling within the dashed box ($\pm 0.5‰$) are considered to be isotopically indistinguishable from their matrix. Tie-lines connect analyses of successive (*arrows*) vein generations determined by cross cutting relationships in a given outcrop. Square symbols are data from Dietrich et al. (1983). (Note that individual isotopic values for this figure have not been rounded as for Table 2)

fluid phase was isotopically buffered by the host carbonates under closed system conditions. Minor excursions from isotopic compliance of vein-matrix pairs can be explained by isotopic exchange of pore waters with clays and carbonaceous materials in the carbonate sediments. These results support microstructural evidence for local scale pressure solution-precipitation, in which the sites of dissolution at grain boundaries or in stylolites are generally close to the veins. Long range transport across different lithological boundaries would certainly have resulted in larger isotopic differences than are observed (see Fig. 5).

Veins and 'dikes' in open systems

In contrast to the majority of veins discussed above, which are isotopically buffered by their matrix, there is a separate population of veins (not represented in Fig. 6) characterized

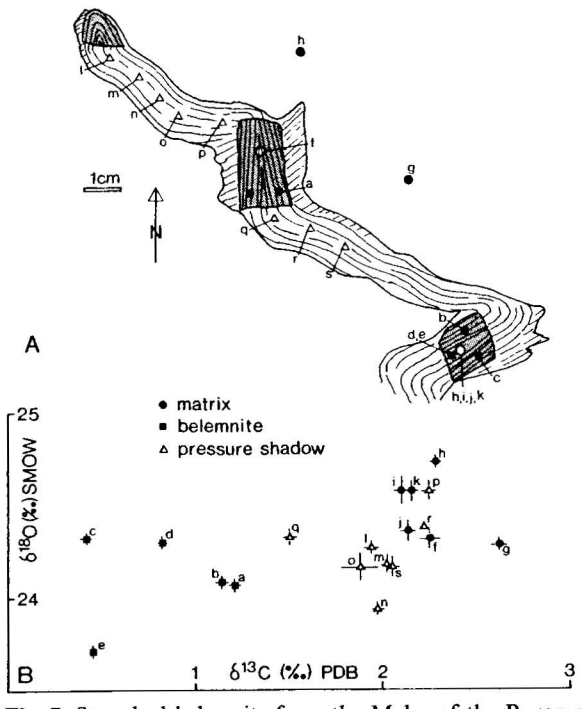

Fig. 7. Stretched belemnite from the Malm of the Raron syncline (sample no. 42). Letters indicate sample spots for isotope analyses. Open circles are from the reverse side of the sample which is a 2 cm thick plate. **B** Isotopic composition of different samples from the matrix, the belemnite and the fibrous pressure shadow. Letters correspond to the spots indicated in **A**. Bars represent two standard deviations of the analytical uncertainity for individual analyses

by isotopic compositions which plot clearly outside of the "marine carbonate field": Sample 32 is a 40 cm thick hydrothermal 'dike' of pure white calcite within the Malm of the Doldenhorn nappe and belongs geometrically to the Type III generation of veins. The calcite is crystallized in equigranular grains of 0.5 to 5 mm and shows intense twinning. The $\delta\ ^{18}O$ value of this 'dike' is unusually low at ca. 1‰, depleted by ca. 23‰ relative to the marine carbonates; but is similar in $\delta\ ^{13}C$. The temperature of formation is not well constrained but assuming a range of isotopic equilibration temperatures between 200 and 350° C, then the $\delta\ ^{18}O$ of H_2O from which the calcite precipitated, or last exchanged, would have been −9‰ (200° C) to −5‰ (350° C) (Fig. 8), signifying involvement of low ^{18}O meteoric surface waters.

A quartz-'dike' (sample 33) within the Tertiary of the Doldenhorn-nappe is geometrically comparable to the calcite-'dike'. The quartz has an unusual texture (Fig. 2E), minor constituents are fluorite, sericite and calcite. Some silicified rock-fragments containing strongly altered biotite are clearly derived from the crystalline basement, and must have been transported over more than 2 km vertically from the underlying Aarmassif. Furrer and Hügi (1952) interpreted this 'dike' as of "telemagmatic" origin. The $\delta\ ^{18}O$ values of the quartz (18.5‰) and calcite (13.9 to 15.8‰) from this 'dike' are clearly different from the "marine carbonate field" (Fig. 4). Quartz-calcite fractionations correspond to calculated isotopic temperatures of 100 to 200° C (Fig. 9). This estimate relies on extrapolation of the quartz-water equation below the limits of calibration, and there is no way of testing for retention of isotopic equilibrium. For an assumed range of temperatures, the $\delta\ ^{18}O$ of water in equilibrium with quartz would have been 5‰ (200° C) to 13‰ (350° C) (Fig. 10).

The calcite and quartz 'dikes' share a common geometry, style of emplacement and timing. These structures show evidence for infiltration of external fluid reservoirs and transport of fluids and solutes over distances of several km. The age and depth of formation is not well defined in either case, and a relatively late near-urface crystallization of the calcite cannot completely be ruled out. Given the retrograde solubility of calcite, the calcite 'dike' may record downward infiltration of fluids undergoing heating (Holland and Malinn 1979). Alternatively, precipitation of large quantities of calcite could be accounted for by unmixing of CO_2 from hydrothermal solutions. Both the quartz and calcite 'dikes' record ^{18}O shifts in the same direction away from the marine carbonate field and syntectonic veins, albeit by differing magnitudes. Further, as discussed above, considerations of fracture mechanics point towards fluid pressures greater than the hydrostatic gradient. The range of estimated $\delta\ ^{18}O$ H_2O values for the quartz 'dike' is not alone diagnostic of a specific hydrothermal fluid reservoir, and magmatic, metamorphic or isotopically evolved formation brines could have been involved or some mixture of these reservoirs. Signifcantly lower calculated $\delta\ ^{18}O$ values of fluids which precipitated the calcite 'dike' require some low ^{18}O meteoric fluid, and meteoric water may have been involved in both systems. This problem is the subject of ongoing studies.

Pressure shadows

The isotopic values measured for fibrous calcite from pressure shadows all lie within the "marine carbonate field", and are also in close compliance with their adjacent matrix. This is anticipated from the microstructural evidence that the pressure shadows are a local phenomenon of pressure solution precipitation over a centimetre scale.

Pressure shadows are well developed in a boudinaged belemnite from a highly deformed Malm limestone of the Raron syncline (Fig. 7). The originally micritic limestone, now a completely recrystallized matrix, retains an isotopic composition which is indistinguishable from less metamorphosed and deformed counterparts of the same unit. Several samples from various spots of this specimen show minor degrees of variability in the isotopic composition (Fig. 7). The isotopic composition of the secondary fibres in the pressure shadow plot between the values for the belemnite and the matrix, but are closer to the latter. This could be accounted for by a larger contribution of calcite to the shadow from pressure dissolution of the deforming matrix than from the rigid belemnite.

Thrusts

Intensely tectonized samples from major Helvetic thrust planes vary considerably in their oxygen isotopic composition. Mylonites from the Diablerets and Morcles thrusts (sample 54 and 55) plot entirely within the field of "marine carbonates" whereas mylonites of the Doldenhorn thrust yield $\delta\ ^{18}O$ values between 15.3 and 25.8‰ (sample 53a–h). A similar range of values is also found for the Lochseiten calc-mylonite from the Glarus overthrust (11.0 to 26.4‰, sample 56 and 57).

The shift in ^{18}O by up to 15‰ relative to the "marine carbonates field" indicates that these mylonites exchanged

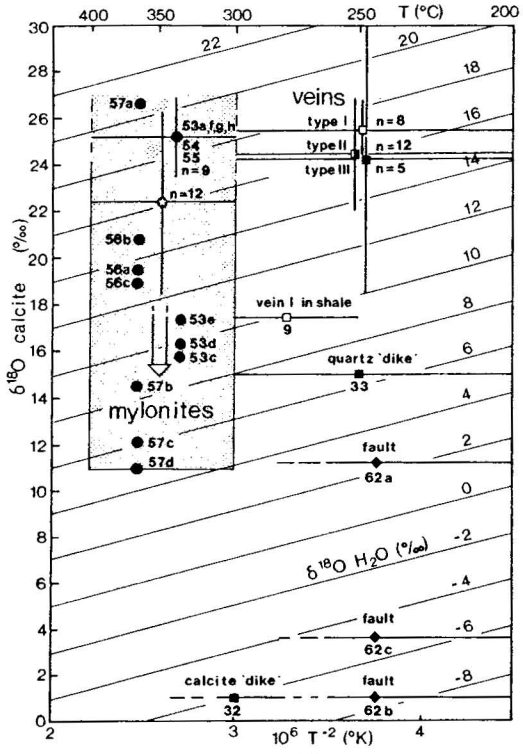

Fig. 8. Measured individual δ ^{18}O calcite values or ranges of values for selected calcites from specified generations of structures plotted versus the estimated temperature of formation. The family of diagonal lines represents δ ^{18}O H_2O in equilibrium with compatible values of δ ^{18}O calcite and temperature according to the calcite-H_2O equation of O'Neil et al. (1969). Symbols are as in Fig. 9. Horizontal lines are the estimated temperature range of a given structure, vertical lines represent two standard deviations of the mean δ ^{18}O value, n is the number of data

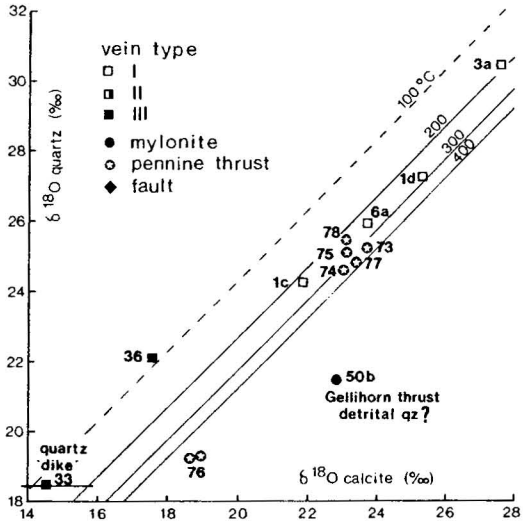

Fig. 9. Plot of δ ^{18}O quartz versus δ ^{18}O of coexisting calcite from specified vein types. The family of diagonal lines are temperatures corresponding to equilibrium quartz-calcite fractionations, constructed from the mineral-H_2O equations of Clayton et al. (1972) and O'Neil et al. (1969). The dashed 100° C was calculated by extrapolating the quartz-H_2O equation below the lower limiting temperature of calibration and accordingly is approximate

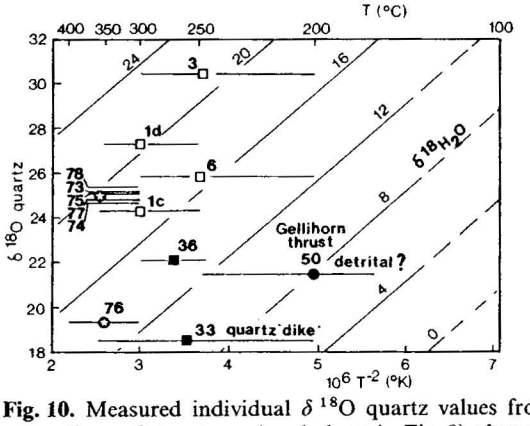

Fig. 10. Measured individual δ ^{18}O quartz values from specified generations of structures (symbols as in Fig. 9) plotted versus the estimated temperature of formation. The family of diagonal lines represents δ ^{18}O H_2O in equilibrium with compatible values of δ ^{18}O quartz and temperature according to the quartz-H_2O equation of Clayton et al. (1972). Horizontal lines are the estimated temperature range of a given structure. Quartz in sample 50 from the Gellihorn thrust is probably of detrital origin

with isotopically light water, unbuffered by the precursor marine carbonates. For the dolomite-rich samples 53a and 56c, calcite-dolomite thermometry (Powell et al. 1984) yields temperatures of 340 and 355 $\pm$ 25° C respectively. These temperatures correspond well to the epizonal grade determined in these areas independently by Frey et al. (1980). Assuming an ambient deformation temperature of 300 to 400° C, the δ ^{18}O of H_2O in equilibrium with mylonites would have been between 4 and 20‰ (Fig. 8).

This spread of calculated δ ^{18}O values for fluids in equilibrium with the Doldenhorn and Lochseiten mylonites is interpreted as a mixing trend. Upper limiting values of about 20‰ likely represent pore fluids isotopically buffered by the marine carbonate derived calc-mylonites, under closed system conditions, as described for most Type I veins. Fluid δ ^{18}O values as low as 4‰ are plausibly isotopically evolved meteoric water, or formation brines (Clayton et al. 1966; for a review see Longstaffe 1987). Thus, the observed spread of calculated δ ^{18}O values of fluids in equilibrium with these mylonites could represent mixtures of limestone buffered pore fluids with either 1) low ^{18}O meteoric surface water infiltrating under hydrostatic conditions, or alternatively 2) with low ^{18}O formation brines expelled under lithostatic conditions from deeper levels along the thrust faults.

Considerations of fluid pressure during thrusting bear critically on this argument. There is a general consensus that translation of large thrust blocks, or nappes, requires fluid pressures approaching lithostatic conditions at the thrust surface, in order to diminish normal stress and thereby reduce the frictional sliding resistance to motion (Hubbert and Rubey 1959; Fyfe et al. 1978). If ambient lithostatic fluid pressures operated during displacement of the Helvetic nappes, then infiltration of hydrostatically pressured low ^{18}O surface water into the mylonites can be ruled out. Variable degrees of isotopic overprinting by low ^{18}O fluids at late stages is considered unlikely because such effects are observed only in the immediate vicinity of large scale open-space fracture fillings. We suggest that during Eocene extensional tectonics, low ^{18}O fluids infiltrated sedimentary aquifers and likely penetrated into the crystalline basement along detachment and transfer faults (cf. Etheridge 1985). In the compressional phase of Alpine tectonics,

Table 2

No	$\delta^{13}C$	$\delta^{18}O$	Mi	Sample description	Coordinates	TE	MET
Type I: (early, schistosity parallel veins)							
1a	0.6	24.0	Cc	vein, 5 mm	613.3/138.1	DH	epi
b	−0.2	18.7	Cc	matrix, Malm limestone	613.5/137.4	DH	
c		24.3	Qz	vein, 5 cm	Gemmipass	DH	220[c−d]
	1.8	25.3	Cc			DH	
d		27.3	Qz	vein, 10 cm		DH	290[a−c]
	1.9	23.8	Cc			DH	
2a	2.4	25.3	Cc	vein, 5 cm	613.5/137.4	DH	epi
b	2.2	25.8	Cc	matrix, Dogger marl	Leukerbad	DH	
3a	2.3	27.6	Cc	vein, 10 cm, fibrous	616.2/144.7	DH	anc
		30.4	Qz	quartz and calcite	Stock	DH	190[a−c]
b	2.4	27.7	Cc	matrix, Valang. marl		DH	
4a	1.2	26.6	Cc	vein, 2 cm	616.9/145.1	DH	anc
b	1.3	26.6	Cc	matrix, Valang. marl	Waldhaus	DH	
5a	2.1	26.7	Cc	vein, 5 mm	617.0/129.0	JA	epi
b	1.6	25.4	Cc	matrix, Malm limestone	Leuk	JA	355[c−d]
6a	1.8	23.7	Cc	vein, 5 cm	669.8/178.2	AU	epi
		25.9	Qz	fibrous quartz	Tellistock	AU	260[a−c]
b	1.4	24.5	Cc	matrix, Malm limestone		AU	
7a	1.2	25.5	Cc	vein, 3 cm	669.8/178.2	AU	epi
b	−0.7	25.3	Cc	matrix, Malm limestone	Tellistock	AU	
8a	1.3	23.9	Cc	vein, 3 cm		AU	epi
b	1.6	24.3	Cc	matrix, Malm limestone		AU	
9a	1.0	17.5	Cc	vein, 1 cm, in	610.6/135.1	WH	anc
	−1.1	15.3	Do	Aalenien black shale	Trubelstock	WH	
b	−0.4	17.0	Cc	vein, 2 mm		WH	
10a	2.1	26.4	Cc	Urgonian limestone	630. /179.	WH	dia
−h	±0.5	±0.7	$n=8$		Sieben Hen.	WH	
Type II: (veins at high angle to schistosity and bedding)							
20a	2.8	24.9	Cc	vein, 3 mm	613.3/138.1	DH	epi
b	2.0	23.3	Cc	vein, 1 cm	Gemmipass	DH	
c	2.5	25.2	Cc	matrix, Malm marl		DH	
21a	1.4	24.1	Cc	vein, 1 cm	611.4/135.4	DH	anc
b	1.7	24.0	Cc	matrix, Tert. shale	Truble	DH	
22a	0.5	25.1	Cc	vein 1, 1 cm	616.3/146.5	DH	anc
b	0.6	25.4	Cc	vein 2, 5 mm	Stock	DH	
c	0.3	25.0	Cc	matrix, Valang. marl		DH	
23a	1.9	28.4	Cc	vein, 5 cm	616.9/145.1	DH	anc
b	1.9	28.2	Cc	matrix, Val. limestone	Waldhaus	DH	
24a	2.3	25.1	Cc	vein, 5 mm	617.0/129.0	JA	epi
b	2.5	25.4	Cc	matrix, Malm limestone	Leuk	JA	
25a	0.5	26.2	Cc	vein 1, 2 cm	608.5/152.6	WH	dia
b	0.1	25.2	Cc	matrix, Hauterivian	Mitholz	WH	
	0.5	26.5	Cc	"Kieselkalk"		WH	
26a	0.5	26.6	Cc	vein 2, 1 cm	608.5/152.6	WH	dia
b	0.6	26.8	Cc	matrix, Hauterivian	Mitholz	WH	
27a	2.1	25.3	Cc	vein, 3 cm	609.6/138.3	WH	anc
b	1.9	25.3	Cc	matrix, Malm limestone	Lämmerenh.	WH	
28a	1.5	23.4	Cc	vein, 2 cm	606.0/131.1	WH	anc
b	1.9	23.8	Cc	matrix, Dogger limestone	Montana	WH	
Type III: (late tensile veins, perpendicular to fold axes)							
30a	1.9	26.3	Cc	vein, 4 cm	616.9/145.1	DH	anc
b	1.9	28.2	Cc	matrix, Val. limestone	Waldhaus	DH	
31a	1.9	26.9	Cc	vein, 1 cm	616.9/145.1	DH	anc
b	1.9	28.2	Cc	matrix, Val. limestone	Waldhaus	DH	
32a	−1.0	0.8	Cc	calcite-'dike', 40 cm	618.5/144.4	DH	epi
b	0.1	9.0	Cc	in Malm limestone	Balmhornhütte	DH	
c	−0.5	0.6	Cc			DH	
d	−0.5	1.4	Cc			DH	
e	−0.5	0.6	Cc			DH	
f	−0.5	0.6	Cc			DH	
33a	0.7	14.3	Cc	quartz-'dike', 3 m,	610.9/135.1	DH	anc
b	0.9	14.9	Cc	in Tertiary	Truble	DH	
	0.7	15.1	Do	limestone		DH	

Table 2

No	$\delta^{13}C$	$\delta^{18}O$	Mi	Sample description	Coordinates	TE	MET
c	1.3	15.8	Cc			DH	100–
d	1.0	13.9	Cc			DH	200[q–c]
		18.5	Qz			DH	
34a	1.5	25.4	Cc	vein, 5 mm	607.9/132.0	WH	anc
b	1.6	24.9	Cc	matrix, Val. limestone	Aminona	WH	
35a	0.9	24.1	Cc	vein, 15 cm	607.3/129.8	WH	anc
b	0.7	24.3	Cc	matrix, Val. marl	Mollens	WH	
36a		22.1	Qz	vein, 15 cm, Dogger	606. /140.	WH	anc
	1.1	17.6	Cc		Truble	WH	
Pressure shadows							
40a	2.8	25.8	Cc	pyrite-halo, 1 cm	619.2/143.9	DH	epi
b	2.8	26.0	Cc	matrix, Malm limestone	Balmhornhütte	DH	
41a	2.4	25.4	Cc	belemnite-halo, 1.5 cm	619.3/144.0	DH	epi
b	2.5	25.8	Cc	matrix, Malm limestone	Balmhornhütte	DH	
42a	1.3	24.1	Cc	belemnite	624.9/130.2	AU	epi
–f	±0.8	±0.2	$n=6$	details see Fig. 8	Hohtenn	AU	
g–k	2.3	24.5	Cc	matrix, Malm limestone		AU	
	±0.2	±0.2	$n=7$			AU	
l–s	2.0	24.3	Cc	fibrous pressure		AU	
	±0.2	±0.3	$n=9$	shadow		AU	
43a	0.7	25.0	Cc	pyrite-halo, 5 mm	605.5/131.1	WH	epi
b	0.6	25.0	Cc	matrix, Val. marl	Montana	WH	
Tectonites							
50a	0.8	25.1	Cc	tectonite boudin	616.4/146.9	GH	dia
	−0.9	20.6	Do	pressure solution,	Kandersteg	GH	
b	−0.2	22.8	Cc	and veins		GH	
		21.5	Qz	detrital?		GH	
51a	−0.5	23.5	Cc	tectonite boudin	613.5/143.0	WH	dia
	−5.2	22.6	Do		Ueschinen	WH	
52a	−2.4	17.5	Cc	tectonite	598.7/125.0	WH	dia
53a	2.5	23.4	Cc	calc-mylonite	620.9/143.9	DH	epi
	2.7	22.2	Do	dynamically	Gasterntal	DH	340[c–d]
b	0.6	15.4	Cc	recrystallized		DH	
c	1.2	15.3	Cc			DH	
d	1.8	16.2	Cc			DH	
	0.4	15.8	Do			DH	
e	0.8	17.3	Cc			DH	
f	2.1	25.7	Cc			DH	
g	2.1	25.4	Cc	syn-mylonitic vein		DH	
h	2.3	25.8	Cc	syn-mylonitic vein		DH	
54a	1.6	25.3	Do	tectonite	584.9/117.1	DI	epi
b	1.7	25.0	Cc	strongly deformed,	Ardon	DI	
	1.6	25.2	Do	dynamically recrys-		DI	
c	1.6	25.3	Cc	tallized limestone		DI	
55a	−1.3	24.1	Cc	calc-mylonite	579.6/113.3	MO	epi
b	1.2	25.0	Cc	dynamically	Saillon	MO	
c	2.4	22.1	Cc	recrystallized		MO	
56a	0.9	19.6	Cc	"Lochseitenkalk"	749.8/205.8	GL	epi
b	1.7	20.7	Cc	calc-mylonite with	Pizol	GL	355[c–d]
c	0.9	18.7	Cc	synmylonitic		GL	
	0.0	17.9	Do	veinlets		GL	
57a	2.1	26.4	Cc	"Lochseitenkalk"	739.4/193.6	GL	epi
b	1.4	14.7	Cc	calc-mylonite	CrapdaFlem	GL	
c	−5.5	12.0	Cc	dynamically		GL	
d	0.2	10.9	Cc	recrystallized		GL	
Late faults							
60a	2.5	22.6	Cc	fault-gouge,	610.5/138.8	WH	anc
b	2.6	23.9	Cc	sparry calcite	Lämmernh.	WH	
c	2.5	23.1	Cc	along fault plane		WH	
d	1.6	24.5	Cc	in Malm limestone		WH	
61a	1.8	24.3	Cc	cataclasite along-	604.5/138.7	WH	dia
b	1.3	21.5	Cc	major fault	Retzligl.	WH	

Table 2

No	$\delta^{13}C$	$\delta^{18}O$	Mi	Sample description	Coordinates	TE	MET
c	1.9	23.6	Cc			WH	
d	1.2	20.0	Cc			WH	
62a	−0.4	11.2	Cc	fault-gouge	669.8/178.2	AU	epi
b	−0.3	1.0	Cc	Cc-slickenfibers	Tellistock	AU	
c	−0.3	3.7	Cc	in Malm limestone		AU	
d	0.5	9.9	Cc	along major fault		AU	
e	1.4	24.5	Cc	matrix, Malm limestone		AU	
Veins related to frontal pennine thrust							
70a	−2.3	20.9	Cc	vein, 2 mm	598.9/124.1	ZS	epi
b	−2.1	25.7	Cc	matrix, carbonate	St. Léonard	ZS	
71a	1.1	22.1	Cc	Trias tectonite	598.9/124.0	ZS	epi
b	0.9	20.6	Cc	tectonite	St. Léonard	ZS	
	1.3	21.5	Do			ZS	
72a	−2.4	20.5	Do	vein, 3 mm	598.9/124.0	ZS	epi
	−2.5	19.6	Do		St. Léonard	ZS	330^{c-d}
b	−2.0	26.2	Do	matrix, Trias dolo.		ZS	
	−2.1	25.0	Do			ZS	
	−2.5	24.8	Cc			ZS	
73a	0.6	23.7	Cc	vein I, 15 cm	633.0/127.2	ZS	epi
	1.3	22.3	Do	boudinaged	Visp	ZS	
		25.2	Qz			ZS	380^{q-c}
74a	1.0	23.0	Cc	vein I, 10 cm		ZS	
	1.2	23.0	Do	folded, boudin.		ZS	370^{c-d}
		24.6	Qz			ZS	350^{q-c}
b	1.0	23.0	Cc	matrix, calc-schist		ZS	
	1.1	22.7	Do			ZS	
75a	1.2	23.1	Cc	vein I, 15 cm	600.7/123.6	ZS	epi
	1.4	22.9	Do	boudinaged	St. Léonard	ZS	345^{c-d}
		25.1	Qz			ZS	300^{q-c}
b	1.0	21.1	Do	matrix, calc-schist		ZS	
	1.0	21.7	Cc			ZS	
76a	−11.0	18.6	Cc	vein I, 10 cm		ZS	epi
	−11.3	18.8	Cc	boudinaged	Sierre,	ZS	$>500^{q-c}$
	−11.5	17.4	Do		(Mangol)	ZS	
	−11.7	16.4	Do			ZS	
		19.3	Qz			ZS	
77a	0.8	21.7	Do	vein I, 5 cm	598.1/123.0	ZS	epi
	1.2	23.4	Cc	boudinaged	St. Léonard	ZS	360^{q-c}
		24.8	Qz			ZS	
78a	0.8	21.7	Do	vein I, 8 cm		ZS	epi
	1.3	22.9	Cc	folded		ZS	
		25.4	Qz			ZS	250^{q-c}
b	0.7	21.7	Do	matrix, calc-schist		ZS	
	1.3	22.9	Cc			ZS	

$\delta^{13}C$ in ‰ PDB, $\delta^{18}O$ in ‰ SMOW, Cc = Calcite, Do = Dolomite, Qz = quartz
TE = tectonic units: AU = Autochthonous, DH = Doldenhorn nappe, MO = Morcles nappe, JA = Jägerchrüz and Plammis imbricates, GH = Gellihorn nappe, DI = Diablerets nappe, WI = Wildhorn nappe, GL = Glaris thrust (eastern Switzerland), ZS = Zone Sion Courmayeur (Frontal pennine thrust zone)
MET = metamorphic grade determined by illite crystallinity and other methods (Burkhard 1988): dia = diagenetic, T = 100–200° C; anc = anchi-zone, T = 200–300° C; epi = epi-zone, T > 300° C. 330^{c-d} = calcite-dolomite thermometry according to (Powell et al. 1984); 330^{q-c} = isotopic temperature from quartz-H_2O and calcite-H_2O fractionation factors (Calyton et al. 1972 and O'Neil et al. 1969)
Coordinates and localities are according to Swiss topographic maps

these low ^{18}O formation brines were expelled from the sediments and basement by tectonic compaction, preferentially along shear zones that propagated as thrust faults into the sedimentary cover. According to Cathles (1983) formation brines may be expelled from sedimentary basins by compaction/tectonics and there is isotopic evidence that some of the expelled brines have undergone isotopic exchange with basement rocks (J- type Pb). A reconnaissance Sr-isotope study has shown that mylonites are variably more radiogenic than undeformed precursors, thus providing corroborative evidence that low $\delta^{18}O$ fluids expelled along the thrusts were derived in part from the basement (Burkhard and Kerrich unpublished data).

In summary, calc-mylonites from the Doldenhorn and Glarus thrusts show evidence for open system fluid advection. Additional analyses are required to determine the precise fluid sources, distances of transport of fluids and solutes, and whether or not these structures acted as major conduits for foreland oriented fluid flow ("squeegee effect", Oliver 1986).

Frontal pennine thrust

Isotopic composition of carbonates from veins of the frontal Pennine units in the Rhone valley show a large scatter (Fig. 4). The $\delta\,^{13}C$ and $\delta\,^{18}O$ values span -11.7 to $+1.4‰$ and 16.4 to 26.3‰ respectively. The range of $\delta\,^{18}O$ values is similar to that determined for Helvetic veins and thrusts. Sample 76 shows a marked depletion in $\delta\,^{13}C$ of more than 10‰ with respect to any other sample. The most plausible source for isotopically light CO_2 is oxidation of organic material given that this particular vein formed in a competent sliver of carboniferous sediment (conglomerate, shales including some anthracite) which was tectonically emplaced in a thick series of gypsum.

Samples 70 to 75 and 77, 78 plot close to the field of marine carbonates but are slightly depleted in ^{18}O. Most of the Pennine carbonate series are of Triassic age and according to Hoefs (1973, p.97) this apparent depletion could be an original feature. On the other hand, the Pennine nappes in this area are dominated by schists and it is possible that the isotopic composition of the veins is also influenced by oxygen isotope exchange with detrital silicate minerals.

Isotopic fractionations between several quartz-calcite pairs in the Pennine thrust yield caculated temperatures of 250 to 380° C (samples 73 to 78, Fig. 9). With the exception of sample 76 which yields unrealistically high temperatures, the mid part of this range is consistent with temperatures obtained by calcite-dolomite thermometry (Powell et al. 1984) which converge at 350° C (Table 2). As this area lies within the lower greenschist facies (Frey 1986), veining probably took place close to peak metamorphic conditions.

Faults

Cataclasites from the Rawil depression are only marginally depleted in ^{18}O relative to the marine carbonate field. In contrast, sample 62a–e are from a large normal fault in the autochthonous cover of the Aarmassiv, which extends over a 2 km vertical interval from the Tertiary down to the crystalline basement. Slickenfiber- and gouge-calcites vary from 1.0 to 11.2‰ in $\delta\,^{18}O$, providing evidence for infiltration of meteoric water into this fault zone (Fig. 8). From microstructural evidence (slicken-fibres) a sub-recent crystallization can be ruled out.

Conclusions

The principal conclusions of this study are as follows:

1) During nappe formation and their emplacement, syntectonic veins and pressure shadows formed under approximately closed system conditions where the isotopic composition of the water was buffered by the surrounding marine carbonate matrix. This result is compatible with microstructural evidence for a pressure solution/precipitation mechanism of deformation responsible for the vein formation.

2) In contrast to closed system conditions within the different nappes, evidence for open system fluid advection is found along the Doldenhorn and Glarus thrust planes. Mixtures of rock buffered pore fluids with low ^{18}O formation brines tectonically expelled from the basement and sediments are the most probable source of variably ^{18}O-depleted water which exchanged with the limestone tectonites.

3) During the later stages of the tectonic evolution, which is marked by 5 to 15 km of uplift and doming of the external crystalline massifs, deep penetration of surface-derived ^{18}O-depleted meteoric water occured along faults, and into the largest of the late tectonic tension fractures.

In summary, closed and open system fluid behaviour coexisted during the main deformation and nappe emplacement. The overall tendency is from closed in the early stages to more open system advection in the later stages of the tectonic evolution, when the deformation processes shifted toward more brittle behaviour diminished lithostatic pressures and enhanced hydraulic conductivity.

Acknowledgements. The authors thank E McLarty and B Edwards for analytical assistance, D Pezderic for conducting the isotopic analyses of quartz and WS Fyfe and JP Schaer for helpful discussions. WS Fyfe provided incisive critique of a provisional draft, and J Mullis and an anonymous referee critically reviewed the manuscript. This study was supported by a post doctoral fellowship of the Fonds National Suisse (N° 2.837-0.85) to MB, and by an NSERC operating grant to RK. The mass spectrometre laboratory at the University of Saskatchewan is partially funded by an NSERC Infrastructure Grant.

References

Baertschi P (1957) Messung und Deutung relativer Häufigkeitsvariationen von ^{18}O und ^{13}C in Karbonatgesteinen und Mineralien. Schweiz Mineral Petrogr Mitt 37:73–152

Burkhard M (1986) La déformation des calcaires de l'Helvétique de la Suisse occidentale (Phénomènes, mécanismes et interprétations tectoniques). Revue Géol dyn Géogr phys 27/5:281–301

Burkhard M (1988) L'Helvétique de la bordure occidentale du massif de l'Aar (Evolution tectonique et métamorphique). Eclogae Geol Helv 81/1:63–114

Cathles LM (1983) An analysis of the hydrothermal system responsible for massive sulfide deposition in the Hokuroku Basin of Japan. Econ Geol Mono 5:439–487

Clayton RN, Mayeda TK (1963) The use of bromine pentafluoride in the extraction of oxygen from oxides and silicates for isotopic analysis. Geochim Cosmochin Acta 27:43–52

Clayton RN, Friedman I, Graf DL, Mayeda TK, Meents WF, Shimp NF (1966) The origin of saline formation waters: I isotopic composition. J Geophys Res 71:3869–3882

Clayton RN, O'Neil JR, Mayeda TK (1972) Oxygen isotope exchange between quartz and water. J Geophys Res 77:3057–3067

Dietrich D, Mc Kenzie JA, Song H (1983) Origin of calcite in syntectonic veins as determined from carbon isotope ratios. Geology 11/9:547–551

Durney DW (1972) Deformation history of the Western Helvetic nappes. Ph.D.thesis, Imperial College, London, p 327

Durney DW, Ramsay JG (1974) Incremental strains measured by syntectonic crystal growths. In: DeJong KA, Scholten R (eds) Gravity and tectonics. Wiley, New York pp 67–91

Etheridge MA (1983) Differential stress magnitudes during regional deformation and metamorphism: upper bound imposed by tensile fracturing. Geology 11:231–234

Etheridge MA, Wall VJ, Vernon RH (1984) The role of the fluid phase during regional metamorphism and deformation. J Metamorphic Geol 1:205–226

Etheridge MA, Wall VJ, Cox SF, Vernon RH (1983) High fluid pressures during regional metamorphism and deformation – implications for mass transport and deformation mechanisms. J geophys Res 89/B6:4344–4358

Franck P, Wagner JJ, Escher A, Pavoni N (1984) Evolution des contraintes tectoniques et sismicité dans la région du Col Sanetsch, Alpes valaisannes helvétiques. Eclogae Geol Helv 77/2:383–393

Frey M (1986) Very low grade metamorphism of the Alps an introduction. Schweiz Mineral Petrog Mitt 66:13–27

Frey M, Hunziker JC, O'Neil JR, Schwander HW (1976) Equilibrium-disequilibrium relations in the Monte Rosa Granite, W Alps: petrological, Rb-Sr and stable isotope data. Contrib Mineral Petrol 55:147–179

Frey M, Teichmüller M, Teichmüller R, Mullis J, Künzi B, Breitschmid A, Gruner U, Schwitzer B (1980) Very low grade metamorphism in external parts of the Central Alps: Illite crystallinity, coal rank and fluid inclusion data. Eclogae Geol Helv 73/1:173–203

Furrer H, Hügi T (1952) Telemagmatischer Gang im Nummulitenkalk bei Trublen westlich Leukerbad (Kanton Wallis). Eclogae Geol Helv 45/1:42–51

Fyfe WS, Price NJ, Thompson AB (1978) Fluids in the earth's crust. Elsevier, Amsterdam pp 320

Fyfe WS, Kerrich R (1985) Fluids and thrusting. Chem Geol 49:353–362

Gregory RT, Criss RE (1986) Isotopic exchange in open and closed systems. In: Valley JW, Taylor HP, O'Neil JR (eds) Stable isotopes in high temperature geologic processes. Reviews in Mineralogy. Min Soc Amer vol 16:91–127

Hoefs J (1973, 1987) Stable isotope geochemistry. Springer, Berlin pp 135, 241

Hoefs J, Frey M (1976) The isotopic composition of carbonaceous matter in a metamorphic profile from the Swiss Alps. Geochimica et Cosmochimica Acta 40:945–951

Hoefs J, Stalder HA (1977) The carbon isotope composition of CO_2-bearing fluid inclusions in fissure quartz from the Central Alps. Schweiz Mineral Petrogr Mitt 57:329–347

Hoernes S, Friedrichsen H (1978) Oxygen and hydrogen isotope study of the polymetamorphic area of the Northern Oetztal-Stubai Alps. Contrib Mineral Petrol 67:305–315

Hoernes S, Friedrichsen H (1980) Oxygen and hydrogen isotopic composition of Alpine and Pre-Alpine minerals in the Swiss Central Alps. Contrib Mineral Petrol 72:19–32

Holland HD, Malinn SD (1979) The solubility and occurence of Non-ore minerals. In: Barnes HL (ed) Geochemistry of hydrothermal ore deposits. Wiley, New York, pp 567

Hubbert MK, Rubey WW (1959) Role of fluid pressure in mechanics of overthrust faulting. Geol Soc America Bull 70:155–166

Hudson JD (1977) Stable isotopes and limestone lithification. J Geol Soc London 133:637–660

Hunziker JC, Frey M, Clauer N, Dallmeyer RD, Friedrichsen H, Flehmig W, Hochstrasser K, Roggwiler P, Schwander H (1986) The evolution of illite to muscovite: mineralogical and isotopic data from the Glarus Alps Switzerland. Contrib Mineral Petrol 92:157–180

Kerrich R (1978) An historical review and synthesis of research on pressure solution. Zbl Geol Paläont Teil I, H 5/6:512–550

Kerrich R (1986) Fluid transport in lineaments. Phil Trans R Soc London A 317:219–251

Kerrich R, Beckinsdale RD, Durham JJ (1977) The transition between deformation regimes dominated by intercrystalline diffusion and intracrystalline creep evaluated by oxygen isotope thermometry. Tectonophysics 38:241–257

Kerrich R, Beckinsale RD, Shackelton NJ (1978) The physical and hydrothermal regime of tectonic vein systems: evidence from stable isotope and inclusion studies. Neues Jahrbuch Mineral Abh 131:225–239

Kerrich R, Rehrig W (1987) Large scale fluid motion associated with Tertiary mylonitization and detachment faulting: $^{18}O/^{16}O$ evidence from Pichacho metamorphic core complex Arizona. Geology 15:58–62

Kübler B, Pittion JL, Heroux Y, Charollais J, Weidmann M (1979) Sur le pouvoir réflecteur de la vitrinite dans quelques roches du Jura, de la Molasse, et des Nappes préalpines, helvétiques et penniques. Eclogae Geol Helv 72/2:347–375

Kyser TK (1987) Short course in stable isotope geochemistry of low temperature fluids. Mineral Assoc Canada vol 13: pp. 452

Laubscher HP (1983) Detachment, shear and compression on the Central Alps. In: Contr to the Tectonics and Geophysics of Mountain Chains. Geol Soc Amer Mem 158:191–211

Longstaffe FJ (1987) Stable isotope studies of diagenetic processes. In: Kyser (ed) Short course in stable isotope geochemistry of low temperature fluids. Mineral Assoc Canada vol 13:187–257

Magaritz M (1974) Lithification of chalky limestone: a case study in Senonian rocks from Israel. J Sed Petrol 44:947–954

McCrea JM (1950) The isotopic chemistry of carbonates and a paleotemperature scale. J Chem Phys 18:849–857

Milnes AG, Pfiffner OA (1980) Tectonic evolution of the Central Alps in the cross section St. Gallen – Como. Eclogae Geol Helv 73:619–633

Mugnier JL, Ménard G (1986) Le dévelopement du bassin molassique suisse et l'évolution des Alpes externes un modèle cinématique. Bull Centre Rech Explor Prod Elf Aquitaine 10/1:191–203

Mullis J (1979) The system methan-water as a geologic thermometre and barometre from the external part of the central Alps. Bull Mineral 102:526–536

Mullis J (1987) Fluid inclusion studies during very low grade metamorphism. In Frey M (ed) Low temperature metamorphism. Blackie Glasgow: 162–199

Oliver J (1986) Fluids expelled tectonically from orogenic belts their role in hydrocarbon migration and other geologic phenomena. Geology 14:99–102

O'Neil JR (1987) Preservation of H, C, and O isotope ratios in the low temperature environment. In: Kyser (ed) Short course in stable isotope geochemistry of low temperature fluids. Mineral Assoc Canada vol 13:85–128

O'Neil JR, Clayton RN, Mayeda TK (1969) Oxygen isotope fractionation in divalent metal carbonates. J Chem Phys 51:5547–5558

Pfiffner OA (1982) Deformation mechanisms and flow regimes in limestones from the Helvetic zone of Swiss Alps. J Struct Geol 4:429–442

Poty P, Stalder A, Weisbrod A (1974) Fluid inclusions studies in quartz from fissures of Western and Central Alps. Schweiz Mineral Petrogr Mitt 54/2+3:717–752

Powell R, Condliffe DM, Condliffe E (1984) Calcite-dolomite geothermometry in the system CaCO3-MgCO3-FeCO3: an experimental study. J Metamorphic Geol 2:33–41

Ramsay JG, Huber MI (1983) The techniques of modern structural geology, vol 1, strain analysis. Academic Press, London p 307

Schmid SM (1982) Laboratory experiments on rheology and deformation mechanisms in calcite rocks and their application to studies in the field. Mitt Geol Inst ETH Univ Zürich 241:1–62

Schmid SM, Casey M, Starkey J (1981) The microfabric of calcite tectonites from the Helvetic nappes (Swiss Alps). In: McClay K, Price NJ (eds) Thrust and nappe tectonics. Spec Publ geol Soc London 9:151–158

Secor DT (1965) Role of fluid pressure in jointing. American J Sci 263:633–646

Taylor BE, Bucher-Nurminen K (1986) Oxygen and carbon isotope and cation geochemistry of metasomatic carbonates and fluids – Bergell aureole Northern Italy. Geochim Cosmochim Acta 50:1267–1279

Tucker ME (1983) Diagenesis and origin of Precambrian dolomite: the Beckspring dolomite of eastern California. J Sediment Petrol 53:1097–1119

Trümpy R (1980) Geology of Switzerland. Part I, Wepf Basel, pp 104

Valley JW, Taylor HP, O'Neil JR (1986) Stable isotopes in high temperature geological processes. Reviews in Mineralogy vol 16, Mineral Soc Amer, pp 570

Veizer J, Hoefs J (1976) The nature of 018/016 and C13/C12 secular trends in carbonate rocks. Geochim Cosmochim Acta 40:1387–1395

Weissert H, Bernoulli D (1984) Oxygen isotope composition of calcite in Alpine ophicarbonates: a hydrothermal or Alpine metamorphic signal. Eclogae Geol Helv 77:29–43